^{1}H NMR Study of a Complex between the *lac* Repressor Headpiece and a 22 Base Pair Symmetric *lac* Operator†

R. M. J. N. Lamerichs,‡ R. Boelens,‡ G. A. van der Marel,§ J. H. van Boom,§ R. Kaptein,*,‡ F. Buck,∥ B. Fera,∥ and H. Rüterjans∥

Department of Chemistry, University of Utrecht, Padualaan 8, 3584 CH Utrecht, The Netherlands, Gorlaeus Laboratory, University of Leiden, P.O. Box 9502, 2300 RA Leiden, The Netherlands, and Institut für Biophysikalische Chemie, Johann Wolfgang Goethe-Universität, Theodor-Stern Kai 7, Haus 75A, D-6000 Frankfurt 70, FRG

Received September 15, 1988; Revised Manuscript Received November 28, 1988

ABSTRACT: A complex between the *lac* repressor headpiece and a fully symmetric tight-binding 22 bp *lac* operator was studied by 2D NMR. Several 2D NOE spectra were recorded for the complex in both H_2O and ^2H_2O. Many NOE cross-peaks between the headpiece and DNA could be identified, and changes in the chemical shift of the DNA protons upon complex formation were analyzed. Comparison of these data with those obtained for a complex between the headpiece and a 14 bp half-operator, studied previously [Boelens, R., Scheek, R. M., Lamerichs, R. M. J. N., de Vlieg, J., van Boom, J. H., & Kaptein, R. (1987) in *DNA–ligand interactions* (Guschlbauer, W., & Saenger, W., Eds.) pp 191–215, Plenum, New York], shows that two headpieces form a specific complex with the 22 bp *lac* operator in which each headpiece binds in the same way as found for the 14 bp complex. The orientation of the recognition helix in the major groove of DNA in these complexes is opposite with respect to the dyad axis to that found for other repressors.

The expression of the lactose genes in *Escherichia coli* is regulated by the *lac* repressor which interacts with a specific 20–25 base pair DNA sequence, the *lac* operator. When the *lac* repressor binds to the operator, transcription of the *lac* genes is blocked. Induction occurs when small molecules such as allolactose or isopropyl 1-thio-β-D-galactoside (IPTG)[1] bind to the repressor which then loses affinity for the operator. The *lac* repressor–operator system is biochemically and genetically very extensively characterized (Gilbert & Maxam, 1973; Gilbert & Müller-Hill, 1966; Miller & Reznikoff, 1978; Miller, 1979, 1984). It appears that the DNA binding properties of the repressor reside in the N-terminal domain (*lac* headpiece) and the inducer binding site in the tetrameric core. Methylation protection studies have shown that the *lac* headpiece interacts with the *lac* operator in a way very similar to that of the intact repressor (Gilbert & Maxam, 1973).

At present, the structures of CAP, λ repressor ("cl"), *cro*, and *trp* repressor have been determined by X-ray crystallography (Mckay & Steitz, 1981; Pabo & Lewis, 1982; Anderson et al., 1981; Schevitz et al., 1985). Recently, crystal structures of repressor–operator complexes were reported for 434 repressor and *cro* (Anderson et al., 1987; Wolberger et al., 1988), *trp* repressor (Otwinowski et al., 1988), and λ-cl repressor (Pabo, personal communication). All these repressors have a common helix–turn–helix structural motif which is involved in the recognition of the specific base sequence of the operator (Pabo & Sauer, 1984). For the *lac* repressor, no X-ray structure is available, but the three-dimensional structure of the headpiece consisting of the first 51 N-terminal residues (HP 51) has been determined by NMR (Kaptein et al., 1985). It was shown that the *lac* headpiece also has a helix–turn–helix motif, in agreement with predictions based on sequence homology with other repressors (Matthews et al., 1982).

From an NMR study of the complex of HP 56 with a 14 bp half-operator, a low-resolution structure of this complex was obtained (Boelens et al., 1987a,b, 1988). The most prominent feature of this structure is that the orientation of the recognition helix in the major groove with respect to the dyad axis is reversed compared to that of all other repressor–operator complexes, either seen in the crystal structures (Anderson et al., 1987; Wolberger et al., 1988; Otwinowski et al., 1988; Pabo, personal communication) or inferred from the structure of the dimeric repressors (Weber et al., 1982; Matthews et al., 1982).

It is known that repressors also bind, although weaker, in a nonspecific way to DNA. It has been proposed that this way of binding may play an important role in the process of finding the operator sequence by the repressor (Winter et al., 1981). NMR studies have shown that isolated headpieces also form nonspecific complexes with DNA (Buck et al., 1980). In the presence of the 14 bp operator, it was concluded that the headpiece forms a specific complex but that nonspecific binding occurred as well (Scheek et al., 1983). The kinetic parameters are such that a fast exchange equilibrium between specific and nonspecific complexes results.

The wild-type *lac* operator has two headpiece binding sites and is nearly symmetric. However, a fully symmetric DNA fragment has been found which binds *lac* repressor 8 times more tightly than the wild-type (Simons et al., 1984; Sadler et al., 1983). In this ideal operator, the central GC base pair is missing, resulting in a perfect palindromic DNA fragment with the left half of the wild-type operator symmetrized.

Here we report an NMR study on the 2:1 complex of HP 56 with a 22 bp fully symmetric tight-binding *lac* operator (see

† This work was supported by the Netherlands Foundation for Chemical Research (SON) with financial support from the Netherlands Organization for Scientific Research (NWO) and by a grant from the Deutsche Forschungsgemeinschaft to H.R. (Ru 145/8-1).

‡ University of Utrecht.

§ University of Leiden.

∥ Johann Wolfgang Goethe-Universität.

[1] Abbreviations: IPTG, isopropyl 1-thio-β-D-galactoside; bp, base pair(s); 2D, two dimensional; NOE, nuclear Overhauser effect; HP, headpiece.

0006-2960/89/0428-2985$01.50/0

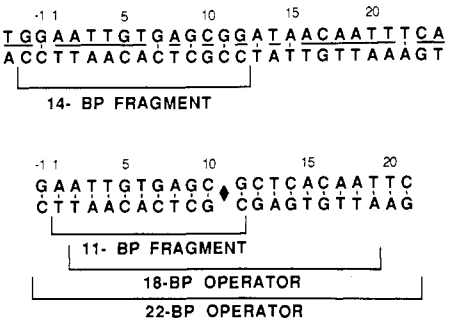

FIGURE 1: Base sequence of the *lac* operator. On top is the sequence of the wild-type operator. Below is that of a tight-binding fully symmetric *lac* operator. Indicated are the various operator fragments discussed in the present study.

Figure 1). It will be shown that the orientation of the recognition helix in this complex is the same as found previously for the 14 bp half-operator.

Experimental Procedures

The 18 and 22 bp DNA fragments were synthesized as described by van Boom et al. (1976) and Kupferschmitt et al. (1987). *lac* repressor was isolated from the *E. coli* strain BMH 74-12 as described previously (Scheek et al., 1983). The *lac* repressor solution in 1 M Tris-HCl, pH 8.0, and 30% glycerol was digested for 4 h at room temperature with 3% (w/w) chymotrypsin A_4 (Arndt et al., 1981). The chymotrypsin was obtained from Boehringer. The HP 56 was purified by gel filtration on a Sephadex G50 column (Pharmacia) followed by a phosphocellulose column (Whatman). Headpiece and DNA were mixed in a 2:1 ratio, and the sample was concentrated and dialyzed on a small-volume Amicon high-pressure cell with YM2 filters (cutoff M_r <1000). The final sample, with a concentration of approximately 4 mM, was in 0.2 M KCl/0.01 M phosphate, pH 6.0.

The NMR spectra were recorded at 500 MHz on a Bruker AM500 interfaced with an Aspect 3000 computer. The data were processed on a MicroVAX II with the "2D NMR" software library written in FORTRAN 77. The two-dimensional (2D) NOE spectra in ^2H_2O were recorded with a 32-step phase cycle (States et al., 1982). The carrier was placed on the HDO signal. The time proportional phase increment (TPPI) method (Marion & Wüthrich, 1984) was used for the t_1 amplitude modulation; 300 free induction decays (FID's) of 2K data points, 64 scans each, were recorded. The t_1 value was incremented from 50 μs to 30 ms. The HDO signal was suppressed by irradiation during the relaxation delay (1.5 s) and during the mixing time. Three spectra with mixing times of 100, 150, and 200 ms were recorded and added in the time domain to improve the signal-to-noise ratio. The time domain data were weighted with a sine bell shifted by $\pi/6$ over the first 1K data points in the t_2 dimension and over all 300 data points in the t_1 dimension. The data were processed to give a phase-sensitive spectrum of 1K × 1 K data points, having a digital resolution of 4.88 Hz/point. Base-line corrections were performed in both the ω_1 and ω_2 domains (Boelens et al., 1985).

For the spectra taken in H_2O, the sample was lyophilized and redissolved in 95% H_2O/5% ^2H_2O. The 2D NOE spectrum was recorded by using the pulse sequence $90°-t_1-90°-t_m-45°-t-45°-t_2$(acq.) with a 200-ms mixing time (t_m). For detection, a $45°-t-45°$ selective pulse was used, which excites the water protons only weakly. To remove unwanted *xy* magnetization, a short field-gradient pulse was given before the selective pulse. The phase cycling was the same as in the

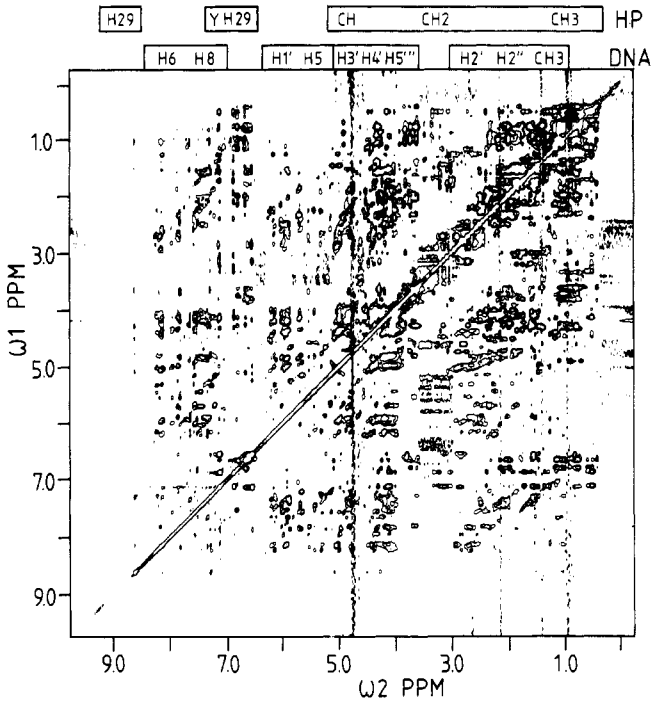

FIGURE 2: ^1H 2D NOE spectrum of the complex between HP 56 and the symmetric 22 bp operator. 500-MHz spectra were recorded of a 4 mM solution of the complex in 0.2 M KCl/0.01 M phosphate, in ^2H_2O, p^{2}H 6.0, 27 °C. The spectrum shown is the sum of three different 2D NOE spectra recorded with mixing times of respectively 100, 150, and 200 ms. The digital resolution is 4.88 Hz/point.

^2H_2O spectra. The carrier was placed between the resonances of the imino protons of the DNA and the H2 proton of His-29, and the imino protons were allowed to fold back; 400 FID's of 64 scans were recorded, and the t_1 value was incremented from 20 μs to 32 ms. The same processing parameters were used as for the 2D NOE spectra taken in ^2H_2O. Again, the spectrum was base line corrected in both frequency domains (Boelens et al., 1985).

Results

Figure 2 shows the 2D NOE spectrum, recorded in ^2H_2O, of the complex of HP 56 with the symmetric 22 bp operator in a stoichiometry of 2:1. Also indicated in this figure are the regions in which the various resonances of both the headpiece and the DNA occur. There are a few windows in the spectrum were there is no overlap between the headpiece and the DNA resonances. These regions have proven to be very useful as starting points for assignments of the resonances.

A part of the spectrum is shown in more detail in Figure 3. This region contains one of the windows, in which only intra-DNA NOE's occur, which were used for the assignment of DNA resonances. The assignments of the H6/H8, H1′, and the cytosine H5 protons of the DNA were made in a very similar way to those of the free operator (Scheek et al., 1985); they are indicated in Figure 3. It should be noted that the H6–H1′ cross-peak of T3 and the sequential cross-peak between the H6 proton of T3 and the H1′ proton of A2 are missing. Previously, it had been assumed that these resonances did not shift but still overlapped with those of T2, as in the spectra of the free operator (Scheek et al., 1985). However, in the spectra of the complex of HP 56 with the 11 bp operator, these cross-peaks, although very weak, were present and provided the correct assignment of the T3 resonances (Boelens et al., 1988). From comparison with these spectra, it was concluded that some cross-peaks of T3 are missing owing to substantial broadening. The correct assignment of the H6 and

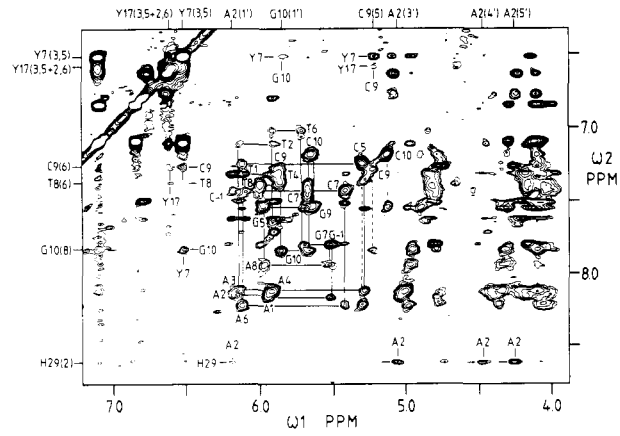

FIGURE 3: Expanded region from ω_2 = 7.3–8.8 ppm and ω_1 = 3.8–7.3 ppm of the spectrum of Figure 2. The sequential assignment of the H6/H8, H1′, and cytosine H5 protons of the symmetric 22 bp operator in the complex with HP 56 is indicated by the lines connecting the NOE cross-peaks. Several NOE's between the operator and the headpiece are also shown.

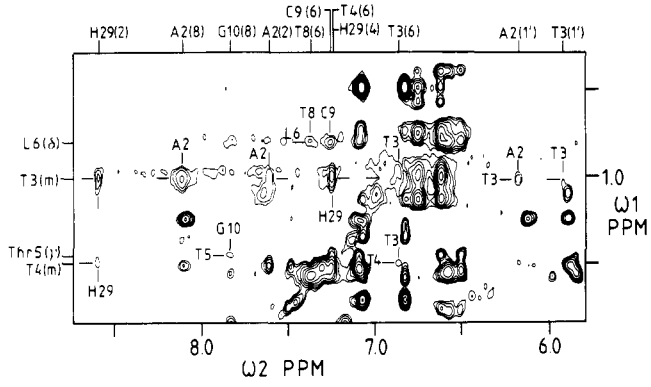

FIGURE 4: Expanded region from ω_2 = 5.8–8.8 ppm and ω_1 = 0.3–1.8 ppm of the spectrum of Figure 2. Assignments of the H6, H1′, and methyl protons of residue T3 of the 22 bp operator in the complex with HP 56 are indicated. The resonances of T3 could be identified by using the sequential cross-peaks between the methyl protons of T3 and the methyl protons of T4 and the H6 proton of A2, respectively. Again, several protein–DNA NOE's are indicated.

H1′ protons of T3 in the spectrum of the HP 56–22 bp complex was possible via its (broadened) methyl resonances (Figure 4). Both the H8 and H1′ protons of A2 have a cross-peak with the methyl protons of T3, as indicated in Figure 4. The resonance position of the H1′ proton of T3 can be found via the intraresidue NOE between the methyl protons and the H1′ proton, while the H6 proton of T3 has an intraresidue NOE with the methyl group and a sequential NOE with the methyl protons of T4. At present, all H6/H8, H1′, and cytosine H5 resonances, all the methyl resonances of the thymines, and most of the H2′ and H2″ sugar protons and some H3′ protons coud be identified in the spectra of the HP 56–22 bp complex.

The assignment of headpiece resonances in the complex with the 14 bp operator was previously done via titrations with operator DNA (Scheek et al., 1983), making use of the fast exchange equilibrium between free and bound headpiece. For a number of nonoverlapping resonances of the 22 bp complex, the assignment was obtained easily in this way since again a fast exchange equilibrium was observed. These included the aromatic ring protons of His-29, Tyr-7, -12, -17, and -47, the aliphatic C_α and C_β protons of Thr-5, and the methyl protons of Leu-6, Val-9, and Leu-45. Since several of these residues (Tyr-47, Leu-6, Val-9, and Leu-45) are buried in the headpiece structure and have characteristic shifts that change only very little upon complex formation, it is reasonable to assume that

Table I: NOE's Observed between Headpiece 56 and the 11, 14, and 22 Base Pair Operators

protein	DNA	11 bp	14 bp	22 bp
	Unambiguous[a]			
Tyr-7 H3,5	–G10 H8	+	+	+
Tyr-7 H2,6	–G10 H8	+		+
Tyr-7 H3,5	–G10 H1′		+	+
Tyr-7 H3,5	–G10 H3′	+	+	+
Tyr-7 H3,5	–C9 H5	+	+	+
Tyr-7 H3,5	–C9 H6	+	+	+
Leu-6 $C_\delta H_3$	–C9 H5	+	+	
Thr-5 $C_\beta H$	–G10 H3′	+		
Tyr-17 H3,5 + H2,6	–C9 H5	+	+	+
Tyr-17 H3,5 + H2,6	–C9 H6		+	+
Tyr-17 H3,5 + H2,6	–T8 H6	+	+	+
His-29 H2	–A2 H8		+	+
His-29 H2	–T3 CH3	+	+	+
His-29 H2	–A2 H1′			+
	Probable[a]			
Thr-5 $C_\gamma H_3$	–G10 H8	+	+	+
Thr-5 $C_\gamma H_3$	–G10 H3′	+	+	
Leu-6 $C_\delta H3$	–C9 H5	+	+	+
Leu-6 $C_\delta H3$	–C9 H6	+	+	+
Leu-6 $C_\delta H3$	–C9 H3′		+	+
Leu-6 $C_\delta H3$	–T8 H6		+	+
Tyr-17 H3,5 + H2,6	–T8 CH3	+	+	
Ser-21 $C_\alpha H$	–T8 CH3	+	+	
Ser-21 $C_\beta H1$	–T8 CH3	+	+	
Ser-21 $C_\beta H2$	–T8 CH3	+	+	
His-29 H2	–A2 H3′	+	+	+
His-29 H2	–A2 H4′	+	+	+
His-29 H2	–A2 H5′[b]	+	+	+
His-29 H2	–A2 H5″[b]	+	+	+
His-29 H4	–T3 CH3	+		+
His-29 H4	–T4 CH3	+	+	
His-29 H2	–T4 CH3	+	+	+

[a] The unambiguous NOE's were assigned at unique resonance frequencies, while the probable NOE's were from resonances which could overlap with resonances of other protons (see test for further discussion). [b] H5′ and H5″ protons were only pairwise assigned.

the headpiece structure basically remains unchanged when operator is bound. On the basis of this assumption, a large number of aliphatic proton resonance could be assigned by using pattern recognition type arguments as explained previously (Boelens et al., 1987b). Since the chemical shifts of the headpiece protons and their NOE cross-peak patterns in the 14 bp complexes and in the present complex were very similar, the assignments of these protons were taken from Boelens et al. (1987a).

Once these assignments were established, NOE's between the headpiece and the DNA could be identified. Some of the protein–DNA NOE's are indicated in Figures 3 and 4. For example, if one extends the horizontal line at 7.85 ppm (of the H8 proton of G10) to low field, a cross-peak is found at 6.51 ppm which can only belong to the 3,5-protons of Tyr-7 (Figure 3). In a similar way, the NOE's of the methyl protons of both T3 and T4 with the C2 proton of His-29 were identified (Figure 4).

A complete list of the protein–DNA NOE's found so far in the HP 56–22 bp operator complex is given in Table I. In addition, the NOE's observed in the complexes with the 11 and 14 bp operator fragments (Boelens et al., 1987a, 1988) are listed. These data will be discussed in more detail below.

For the complexes of HP 56 with the 11, 14, and 22 bp operators, the ^1H chemical shifts of DNA protons both in the free operator and in the complex were measured. The changes in chemical shift upon binding of the headpiece for the H6/H8 protons are shown in Figure 5a, and for the H1′ protons in Figure 5b. The figure shows that the patterns of chemical shift changes for the three operator fragments are very similar. For

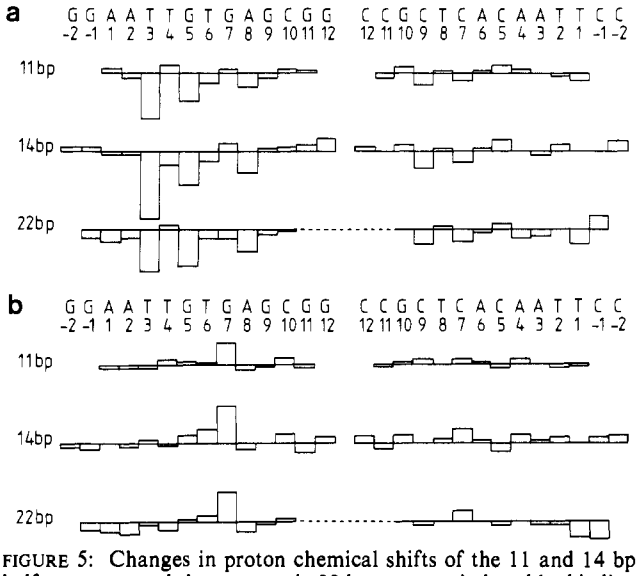

FIGURE 5: Changes in proton chemical shifts of the 11 and 14 bp half-operators and the symmetric 22 bp operator induced by binding of HP 56. (a) Chemical shift differences for the H6/H8 protons and (b) for the H1′ protons. The bars represent the shift differences between the proton resonances in the complex and those of the free operator. The distance between two lines corresponds to 0.4 ppm.

the H6/H8 protons, the large shift difference of T3 (varying from 0.21 to 0.35 ppm for the different complexes) is characteristic. For G5, A8, C9, and C7, similar shift differences are found in all three complexes. For the H1′ protons, the most pronounced shifts are always found at G7 and to a lesser extent at its neighbors. Together with the protein–DNA NOE's from Table I, this similarity in chemical shift changes is an indication that always the same specific binding mode occurs in the various complexes.

We have also looked at complexes of HP 51 with various operator fragments. For complexes of HP 51 with the 22 bp operator and also with a symmetric 18 bp operator, which lacks the base pairs GC-1 and AT-1, the same characteristic changes in chemical shift were found. However, the changes are less pronounced than in the complexes formed with HP 56. In the HP 51–18 bp complex, the resonances of T3 were hardly broadened, and its H6 proton was only shifted 0.10 ppm upfield with respect to the free 18 bp operator. This value is 0.21 ppm in the HP 56–22 bp complex and 0.12 ppm for the HP 51–22 bp complex. Only a few protein–DNA NOE's could be identified, but these are also present in the spectra of HP 56 with the various operators. For the HP 51–22 bp complex, the NOE's of Tyr-7 H3,5 with G10 H8, C9 H5, G10 H1′, and C9 H6 and between the aromatic protons of Tyr-17 and C9 H6 could be observed and for the complex with the 18 bp operator only the first two of these NOE's involving Tyr-7 H3,5. Apparently, specific binding is weaker in these cases. However, both the changes of the chemical shifts and the protein–DNA NOE's show that the type of complex between HP 51 and the symmetric 22 and 18 bp operators is the same as for HP 56 and the 22 bp operator and the 11 and 14 bp half-operators.

For the free 22 bp operator and for its complex with HP 56, NMR spectra were also recorded in H_2O in order to examine the exchangeable protons. A part of the 2D NOE spectrum of the HP 56–22 bp complex in H_2O is shown in Figure 6. As indicated in this figure, each imino proton (except the terminal GC-1) shows an NOE to its neighboring one. This shows that the DNA structure is not drastically disrupted upon complex formation. The assignments of the imino protons in the free 22 bp operator were obtained from

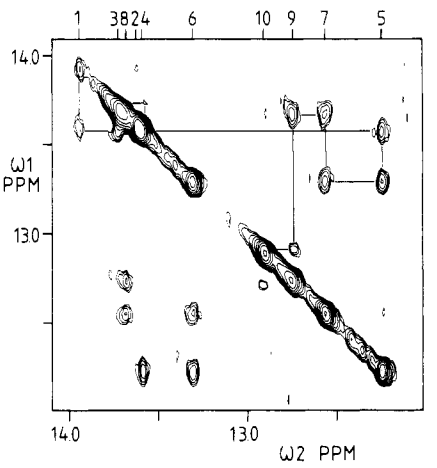

FIGURE 6: Assignment of the imino protons of the symmetric 22 bp operator fragment in a complex with HP 56. Shown is the imino proton region $\omega_2 = \omega_1 = 11.9$–$14.1$ ppm taken from a 2D NOE spectrum recorded for the complex in H_2O. The imino protons are indicated by the numbers at the top of the figure. The assignment is shown by the lines that interconnect cross-peaks.

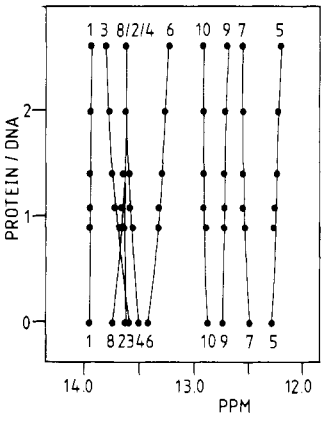

FIGURE 7: Titration shifts of the imino protons of the symmetric 22 bp operator. 500-MHz ^1H NMR spectra were taken at several protein:DNA ratios. The titration was done in 0.2 M KCl, pH 7.0. The concentration of the DNA was 1.6 mM.

1D difference NOE spectra and from 2D NOE spectra in H_2O (data not shown). The imino protons of GC-1 (and of the symmetrically related GC-21) are missing due to fraying effects at the ends of the DNA fragment. In a series of 1D experiments, the imino proton chemical shifts of the 22 bp operator were followed during a titration with HP 56. The results are shown in Figure 7. The chemical shift curves show a typical fast exchange behavior with the largest shifts occurring for the AT imino protons of base pairs 3, 6, and 8. Ambiguities in the assignments in the crossing regions of the curves could be resolved with aid of the assignments in the complex (Figure 6).

Discussion

With a molecular weight of approximately 26 000, the complex of two HP 56 fragments with the symmetric 22 bp operator is among the largest systems studied in detail by NMR. Of course, the analysis was greatly facilitated by the 2-fold symmetry which is preserved in this complex and the fact that the spectra of the constituents had been analyzed previously in great detail (Boelens et al., 1987a,b, 1988).

The changes in chemical shifts measured for the imino protons of the 22 bp operator upon titration with HP 56 (cf. Figure 7) closely resemble the previously determined titration curves for the binding of HP 51 to the 14 bp half-operator

(Scheek et al., 1983). We note that in this previous work uncertainties existed as to the assignments in the complex. With the present results, these data can now be reinterpreted. It appears that also in the case of the HP 51–14 bp complex the imino protons of base pairs 3, 6, and 8 display the largest shifts and those of 1 and 2 shift only very little. From an analysis of the binding curves at various concentrations, it was concluded (Scheek et al., 1983) that in addition to the formation of a specific complex also nonspecific binding must occur. A similar binding curve was observed for the HP 56–22 complex shown in Figure 7 except for the leveling off at a protein to DNA ratio of 2:1 in the present case, rather than 1:1 for the 14 bp complex. This indicates that the NMR measurements presented here pertain to a complex with 2:1 stoichiometry. Again, nonspecific complexes are also present in fast exchange with the specific one. However, since all protein–DNA NOE's, which have been identified so far, can be accounted for in one structural model for the headpiece–operator complex, we conclude that the lifetime of the nonspecific complexes is probably too short to give buildup of NOE intensity.

Concerning the protein–DNA NOE's listed in Table I, a few remarks have to be made. First, a distinction is made between NOE's that are unambiguous because they involve protons with unique resonance positions and those that are probable. The latter occur in crowded regions where overlap of resonance may occur. They were assigned on the basis of a pattern recognition procedure, which involves the following reasoning. Suppose a cross section of a DNA proton shows NOE's to a set of other protons of the same base pair. Then, if a cross section of a headpiece proton shows cross-peaks at the same frequencies and at least one of them can be uniquely assigned to a DNA proton, we consider the assignment of the other cross-peaks in the set also very likely. For example, the C2 proton of His-29 shows a cross-peak to the A2 H1′ proton and a further set of cross-peaks in the DNA ribose region (Figure 3). At the corresponding frequencies, cross-peak intensity is also found at the horizontal line of the A2 H8 proton resonance. Hence, the His-29–DNA cross-peaks are also assigned to the H3′, H4′, H5′, and H5″ protons of A2. Since they occur in a crowded region, they are listed as probable in Table I, while the cross-peak between His-29 H2 with A2 H1′ is uniquely assigned.

Second, a slightly different set of NOE's has been observed for the three HP 56–operator complexes. Differences are mostly due to overlap situations. For instance, the H4 proton of His-29 resonates at a unique frequency in the spectra of the 11 bp and 14 bp complexes but overlaps with the H6 proton of T4 in the 22 bp complex (cf. Figure 4). Therefore, the cross-peak of His-29 H4 with the methyl group of T4, which was observed clearly in the 11 and 14 bp cases, could not be unambiguously identified in the 22 bp spectrum and was not included in Table I. However, the NOE of the T4 methyl group to the H2 proton of His-29 could be identified in the spectra of all three complexes. Therefore, we believe that these differences in the NOE's listed in Table I do not reflect structural differences between the various complexes.

Finally, the protein–DNA NOE's were measured in spectra recorded with rather long mixing times. This was done in order to optimize the intensity of the NOE's and to facilitate the resonance assignments. Therefore, there can be a considerable contribution of spin diffusion to the cross-peak intensities. For instance, the weak protein–DNA NOE's concerning Leu-6 and C9 are probably due to spin diffusion via Tyr-7. We estimate that for strong NOE's the distance between the protons will be less than 4 Å while for the weak ones the distances can be up to 6 Å.

In the experiments carried out with HP 51, we found that the chemical shift changes induced in the 22 bp operator ^1H resonances (data not shown) were qualitatively very similar to those of HP 56 (Figure 5a,b) but smaller. Also, fewer protein–DNA NOE cross-peaks were found. The NOE's that were observed, however, were also seen in the complex with HP 56 (Table I). We conclude, therefore, that HP 51 forms a weaker specific complex than HP 56 and that the peptide segment 52–56 must contribute to specific operator binding. This is in agreement with genetic studies (Miller, 1979, 1984) which showed that replacement of Ala-53 and Gln-54 by other amino acid residues results in I^- mutants that lose operator binding capacity. Since we have found no medium- or long-range intraprotein NOE's beyond Pro-49, we cannot specify the conformation of the C-terminal 50–56 peptide, and, therefore, the molecular basis of the contribution to operator binding of this region remains unknown.

As far as the DNA is concerned the present data show that it stays basically in a B-DNA type conformation. This can be concluded from the following observations. First, the network of interconnecting NOE cross-peaks from which the assignments of the H6/H8 and H1′ protons was obtained (Figure 3) is very similar for free and protein-bound DNA. The same is also true for the imino protons NOE's (Figure 6). Finally, the fact that all imino protons (except the terminal ones) are observable in the spectrum indicates that the double-helical structure is intact because base pair opened conformations would have led to increased exchange with H_2O and broadening or loss of resonance intensity.

It is tempting to interpret the chemical shift changes of the various DNA protons that occur on protein binding, although this cannot be done unambiguously as in the case of NOE's. In general, it can be said that chemical shifts of the imino protons, because of their internal position in the DNA, are more likely to reflect structural changes in the DNA, while the shifts of H6/H8, methyl, and sugar protons may also be affected by the presence of protein side chains. Therefore, minor changes in the structure, such as bending and/or unwinding, could possibly explain the shifts of the imino protons upon complex formation. For the nonexchangeable DNA protons, the chemical shift changes may have similar (structural) origins but can also be induced by the presence of amino acid residue side chains. For instance, the large chemical shift of the H6 proton of T3 could be explained by the presence of the aromatic ring of His-29. Similarly, the shifts of A8 and C9 could be due to the aromatic rings of Tyr-7 and Tyr-17 which are close to this region of the operator. The proximity of charged groups can also cause chemical shift changes. For the HP 56–14 bp complex, a contact of Arg-22 with GC5 was predicted, a possible explanation for the shift of the H8 proton of G5. We note that the H6 proton of T3 and also its methyl group show substantial broadening in the complex. This is due to the fact that these protons, which display the largest shift changes, are not in the fast exchange limit anymore.

The model for the *lac* headpiece–operator complex discussed before (Boelens et al., 1987a,b, 1988) could account for all NOE's identified between HP 56 and the 14 bp operator. The more extensive list of NOE's of Table I can be explained by the same model. Figure 8 shows a model for the complex of the 22 bp operator with two headpieces obtained by symmetrization about the dyad axis of the operator. As mentioned in the introduction, the orientation of the recognition helix (helix II)with respect to the dyad axis is opposite to that in

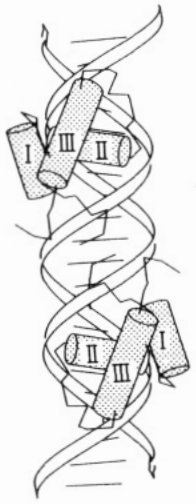

FIGURE 8: Model of the complex between two *lac* repressor headpieces and the symmetric 22 bp operator based on the NMR data. The structure of HP 51, obtained from restrained molecular dynamics (Kaptein et al., 1985), was docked on the 14 bp half-operator (Boelens et al., 1988), using distance constraints derived from interprotein–DNA NOE's (cf. Table I). The structure was obtained from the 14 bp complex by deleting the first two base pairs and symmetrizing about the 2-fold axis.

the models for the *cro*–O_R3 complex (Ohlendorf et al., 1982) and also to that proposed for the *lac* repressor based on the analogy with *cro* (Matthews et al., 1982) and CAP (Weber et al., 1982). It is also opposite to the orientation found in the crystals for the complex of the 434–repressor and its operator (Anderson et al., 1987; Wolberger et al., 1988; Otwinowski et al., 1988; Pabo, personal communication).

In this paper, we showed that the complex of two HP 56 molecules and an ideal 22 bp *lac* operator is fully symmetric and that the specific binding is the same as in the complexes of one headpiece with the 14 and 11 bp half-operators. Because of the large molecular weight of the intact repressor, a detailed study by NMR of complexes even with short *lac* operator fragments is impossible. The intact *lac* repressor is believed to bind to the operator with two headpieces in such way that an approximate 2-fold symmetry axis is present (Kania & Brown, 1976). An important question then is whether the whole *lac* repressor binds to the operator with its headpieces in the same orientation as we have found for isolated headpieces. Recently, genetic experiments carried out in the group of B. Müller-Hill have provided evidence that this is actually the case. Lehming et al. (1987) constructed a *lac* repressor mutant with the first two amino acids of the recognition helix replaced by those of the *gal* repressor (Tyr-17 → Val, Gln-18 → Ala). This mutant repressor had high affinity for the *gal* operator, which differs from the *lac* operator at positions 7 and 9. Although this gives already some clue as to the orientation of the recognition helix, a more definitive result was their finding of a repressor mutant with Arg-22 replaced by Asn, which now had specificity for a *lac* operator with GC5 replaced by TA (Müller-Hill, private communication). This provides support for the Arg-22–GC5 contact in the native system that we predicted on the basis of the NMR results (Boelens et al., 1987a, 1988). It also fixes unambiguously the orientation of the recognition helix as opposite to that of *cro* and λ repressors. It appears, therefore, that there are two classes of helix–turn–helix proteins, which can be generically designated as *lac* and *cro*. From homology arguments and also based on the genetic experiments by Lehming et al. (1987), it appears that at least *gal* and *deo* repressors belong to the *lac* class. The repressors with know crystal structures, λ-cl, *cro*, *trp*, 434 (and the related P 22), and also CAP fall in the *cro* class.

REFERENCES

Anderson, J. E., Ptashne, M., & Harrison, S. C. (1987) *Nature (London) 326*, 846–852.

Anderson, W. F., Ohlendorf, D. H., Takeda, Y., & Matthews, B. W. (1981) *Nature (London) 290*, 754–758.

Arndt, K. T., Boschelli, F., Lu, P., & Miller, J. H. (1981) *Biochemistry 20*, 6109–6118.

Boelens, R., Scheek, R. M. Dijkstra, K., & Kaptein R. (1985) *J. Magn. Reson. 62*, 378–386.

Boelens, R., Scheek, R. M., Lamerichs, R. M. J. N., de Vlieg, J., van Boom, J. H., & Kaptein, R. (1987a) in *DNA–ligand Interactions* (Guschlbauer, W., & Saenger, W., Eds.) pp 191–215, Plenum, New York.

Boelens, R., Scheek, R. M., van Boom, J. H., & Kaptein, R. (1987b) *J. Mol. Biol. 193*, 213–216.

Boelens, R., Lamerichs, R. M. J. N., Rullmann, J. A. C., van Boom, J. H., & Kaptein, R. (1988) *Protein Sequence and Data Analysis* (in press).

Buck, F., Rüterjans, H., Kaptein, R., & Beyreuther, K. (1980) *Proc. Natl. Acad. Sci. U.S.A. 77*, 5145–5148.

Ebright, R. M. (1985) *J. Biomol. Struct. Dyn. 3*, 281–297.

Gilbert, W., & Müller-Hill, B. (1966) *Proc. Natl. Acad. Sci. U.S.A. 56*, 1891–1898.

Gilbert, W., & Maxam, A. (1973) *Proc. Natl. Acad. Sci. U.S.A. 70*, 3581–3584.

Kania, J., & Brown, D. T. (1976) *Proc. Natl. Acad. Sci. U.S.A. 73*, 3529–3533.

Kaptein, R., Zuiderweg, E. R. P., Scheek, R. M., Boelens, R., & van Gunsteren, W. F. (1985) *J. Mol. Biol. 182*, 179–182.

Kupferschmitt, G., Schmidt, J., Schmidt, Th., Fera, B., Buck, F., & Rüterjans, H. (1987) *Nucleic Acids Res. 15*, 6225–6241.

Lehming, N., Sartorius, J., Niemöller, M., Genenger, G., von Wilcken-Bergmann, B., & Müller-Hill, B. (1987) *EMBO J. 6*, 3145–3153.

Marion, D., & Wüthrich, K. (1984) *Biochem. Biophys. Res. Commun. 113*, 967–974.

Matthews, B. W., Ohlendorf, D. H., Anderson, W. F., & Takeda, Y. (1982) *Proc. Natl. Acad. Sci. U.S.A. 79*, 1428–1432.

Mckay, D. B., & Steitz, T. A. (1981) *Nature (London) 290*, 744–749.

Miller, J. H. (1979) *J. Mol. Biol. 131*, 249–258.

Miller, J. H. (1984) *J. Mol. Biol. 180*, 205–212.

Miller, J. H., & Reznikoff, W. (1978) *The operon*, 2nd ed., Cold Spring Harbor Laboratory, Cold Spring Harbor, NY.

Ohlendorf, D. H., Anderson, W. F., Fisher, R. G., Takeda, Y., & Matthews, B. W. (1982) *Nature (London) 298*, 718–723.

Otwinowski, Z., Schevitz, R. W., Zhang, R.-G., Lawson, C. L., Joachimiak, A., Marmorstein, R. Q., Luisi, B. F., & Sigler, P. B. (1988) *Nature (London) 335*, 321–329.

Pabo, C. O., & Lewis, M. (1982) *Nature (London) 298*, 443–447.

Pabo, C. O., & Sauer, R. T. (1984) *Annu. Rev. Biochem. 53*, 293–321.

Sadler, J. R., Sasmor, H., & Betz, J. L. (1983) *Proc. Natl. Acad. Sci. U.S.A. 80*, 6785–6789.

Scheek, R. M., Zuiderweg, E. R. P., Klappe, K. J. M., van Boom, J. H., Kaptein, R., Rüterjans, H., & Beyreuther, K. (1983) *Biochemistry 22*, 228–235.

Scheek, R. M., Boelens, R., Russo, N., & Kaptein, R. (1985) in *Structure and Motion: Membranes, Nucleic Acids and*

Proteins (Clementi, E., Corongui, G., Sarma, M. H., Sarma, R. H., Eds.) pp 485–495, Adenine Press, Guilderland, NY.
Schevitz, R. W., Otwinowski, Z., Joachimiak, A., Lawson, C. L., & Sigler, P. B. (1985) *Nature (London) 317*, 782–786.
Simons, A., Tils, D., von Wilcken-Bergmann, B., & Müller-Hill, B. (1984) *Proc. Natl. Acad. Sci. U.S.A. 81*, 1624–1628.
States, D. J., Haberkorn, R. A., & Ruben, D. J. (1982) *J. Magn. Reson. 48*, 286–297.
van Boom, J. H., Burgers, P. H. J., & van Deursen, P. H. (1976) *Tetrahedron Lett.*, 869–872.
Weber, I. T., Mckay, D. B., & Steitz, T. A. (1982) *Nucleic Acids Res. 10*, 5085–5102.
Winter, R. B., Berg, O. G., & von Hippel, P. H. (1981) *Biochemistry 20*, 6961–6977.
Wolberger, C., Dong, Y., Ptashne, M., & Harrison, S. C. (1988) *Nature (London) 335*, 789–795.
Wüthrich, K. (1986) in *NMR of proteins and nucleic acids*, Wiley, New York.

Proton NMR Studies of a Metallothionein from *Neurospora crassa*: Sequence-Specific Assignments by NOE Measurements in the Rotating Frame†

J. A. Malikayil,‡ Konrad Lerch,§ and Ian M. Armitage*,‡

Departments of Molecular Biophysics and Biochemistry and of Diagnostic Radiology, Yale University School of Medicine, P.O. Box 3333, New Haven, Connecticut 06510, and Biochemisches Institut, Universität Zürich, Winterthurerstrasse 1, CH-8057 Zürich, Switzerland

Received September 13, 1988; Revised Manuscript Received December 6, 1988

ABSTRACT: Sequential ^{1}H NMR assignments of a metallothionein from *Neurospora crassa* have been accomplished by the combined use of COSY, 2QF-COSY, HOHAHA, and rotating-frame NOE experiments. All potentially observable resonances were assigned except for the ϵ-NH_3 group of the C-terminal lysine. ^{1}H NOEs, when observed in the laboratory frame and at 500-MHz spectrometer frequency, were negligible in this protein due to the inherent rotational correlation time of the molecule. This difficulty was circumvented by measuring transverse NOEs in the rotating frame under spin-locking conditions. The observed pattern of NOEs reveals a marked absence of "regular" secondary structures in the protein. Thus, the stability of this metallothionein's tertiary structure must arise primarily from its metal ligation. This appears to be a general feature of MTs since a general lack of extensive secondary structural elements was also observed in other metallothioneins.

Metallothionein from the fungus *Neurospora crassa* (NMT) is the smallest known metallothionein (MT). The protein contains 25 amino acid residues and has a molecular weight (M_r) of 2200. When isolated from mycelia that were exposed to high levels of Cu, NMT contains 6 mol of Cu(I)/mol of protein in thiolate ligation to seven cysteine residues (Beltramini & Lerch 1986). The positions of all seven cysteines are identical with those of the first seven cysteines of the N-terminal region (β domain) of hepatic mammalian MTs. However, NMT binds exclusively Cu(I) in its physiological state in contrast to the β domain of mammalian MTs that are known to accommodate a variety of heavy metal ions (Kägi & Vallee, 1961). Both NMR and X-ray diffraction methods have been used to elucidate the 3D structure of two mammalian MTs (Frey et al., 1985; Braun et al., 1986; Vasak et al., 1987; Furey et al., 1986). A comparable wealth of structural information is not yet available for NMT or for MTs from lower organisms. With the objective to obtaining the same, we have conducted a two-dimensional ^{1}H NMR study of NMT. Of particular interest was the elucidation of the three-dimensional solution structural features of NMT that attribute this protein with its exclusive in vivo specificity for Cu(I). In this paper we describe the complete sequence-specific ^{1}H NMR resonance assignments of the protein.

The use of the conventional two-dimensional nuclear Overhauser experiment (2D NOESY) in this study proved unsuccessful in providing ^{1}H NOEs for sequential resonance assignments. This results from the fact that the tumbling rate τ_c of this protein is such that $\omega\tau_c \sim 1$ at a spectrometer frequency of 500 MHz which results in negligible ^{1}H–^{1}H NOEs in the laboratory frame. Therefore, we used the 2D CAMELSPIN experiment to measure transverse NOEs in the rotating frame under spin-locking conditions (Bothner-By et al., 1984). In the rotating frame, NOEs are always positive and increase with increasing correlation time of the molecule. Rotating-frame NOEs have the additional advantage that the spin-diffusion effects are smaller than those in NOESY spectra (Bothner-By et al., 1984).

Experimental Procedures

Sample Preparation. NMT contains six diamagnetic Cu(I) centers that are susceptible to facile oxidation to the paramagnetic Cu(II) state in the presence of oxygen. The presence of Cu(II) ions can severely hamper the NMR analysis because of line broadening and the consequent quenching of proton NOEs by paramagnetic relaxation. Therefore, special precautions were taken to safeguard the protein from exposure

† This work was supported by a grant from the National Institute of Health, DK 18778, and benefited from instrumentation provided through the shared instrumentation program of the Division of Research Resources of NIH, RR 03475, the Biological Instrumentation Program of the National Science Foundation, DMB 8610557, and the American Cancer Society, RD259. The support of a Swiss National Science grant to K.L. is also acknowledged.

‡ Yale University School of Medicine.
§ Universität Zürich.

0006-2960/89/0428-2991$01.50/0